Optimum heterodyning angle for heterodyned optical Kerr gated ballistic imaging

Shichao Xu,[1] Wenjiang Tan,[1,*] Jinhai Si,[1] Pingping Zhan,[1] Junyi Tong,[2] and Xun Hou[1]

[1]*Key Laboratory for Physical Electronics and Devices of the Ministry of Education & Shannxi Key Lab of Information Photonic Technique, School of Electronic and Information Engineering, Xi'an Jiaotong University, No. 28, Xianning West Road, Xi'an, 710049, China*

[2]*Departments of Applied Physics, Xi'an University of Technology, No. 5, South Jinhua Road, Xi'an, 710048, China*

[*]*tanwenjiang@mail.xjtu.edu.cn*

Abstract: We perform heterodyned optical Kerr gated (HOKG) ballistic imaging of an object hidden behind a turbid medium using a femtosecond laser. The experimental results show that an optimum heterodyning angle should be selected to acquire the highest spatial resolution of the HOKG imaging system. The optimum heterodyning angle depends on the scattering parameters of the turbid media, and it decreases with increasing optical density or decreasing thickness of the turbid medium.

OCIS codes: (190.7110) Ultrafast nonlinear optics; (190.3270) Kerr effect; (320.7160) Ultrafast technology; (290.7050) Turbid media.

References and links

1. L. Wang, P. P. Ho, C. Liu, G. Zhang, and R. R. Alfano, "Ballistic 2-d imaging through scattering walls using an ultrafast optical kerr gate," Science **253**(5021), 769–771 (1991).
2. D. Sedarsky, E. Berrocal, and M. Linne, "Quantitative image contrast enhancement in time-gated transillumination of scattering media," Opt. Express **19**(3), 1866–1883 (2011).
3. M. E. Zevallos L, S. K. Gayen, M. Alrubaiee, and R. R. Alfano, "Time-gated backscattered ballistic light imaging of objects in turbid water," Appl. Phys. Lett. **86**(1), 011115 (2005).
4. W. Tan, Z. Zhou, A. Lin, J. Si, P. Zhan, B. Wu, and X. Hou, "High contrast ballistic imaging using femtosecond optical Kerr gate of tellurite glass," Opt. Express **21**(6), 7740–7747 (2013).
5. M. Linne, D. Sedarsky, T. Meyer, J. Gord, and C. Carter, "Ballistic imaging in the near-field of an effervescent spray," Exp. Fluids **49**(4), 911–923 (2010).
6. J. B. Schmidt, Z. D. Schaefer, T. R. Meyer, S. Roy, S. A. Danczyk, and J. R. Gord, "Ultrafast time-gated ballistic-photon imaging and shadowgraphy in optically dense rocket sprays," Appl. Opt. **48**(4), B137–B144 (2009).
7. D. L. Sedarsky, J. Gord, C. Carter, T. Meyer, and M. A. Linne, "Fast-framing ballistic imaging of velocity in an aerated spray," Opt. Lett. **34**(18), 2748–2750 (2009).
8. S. Idlahcen, L. Méès, C. Rozé, T. Girasole, and J. B. Blaisot, "Time gate, optical layout, and wavelength effects on ballistic imaging," J. Opt. Soc. Am. A **26**(9), 1995–2004 (2009).
9. M. E. Paciaroni and M. Linne, "Single-shot, two-dimensional ballistic imaging through scattering media," Appl. Opt. **43**(26), 5100–5109 (2004).
10. H. Purwar, S. Idlahcen, C. Rozé, D. Sedarsky, and J.-B. Blaisot, "Collinear, two-color optical Kerr effect shutter for ultrafast time-resolved imaging," Opt. Express **22**(13), 15778–15790 (2014).
11. P. Zhan, W. Tan, J. Si, S. Xu, J. Tong, and X. Hou, "Optical imaging of objects in turbid media using heterodyned optical Kerr gate," Appl. Phys. Lett. **104**(21), 211907 (2014).
12. W. T. Lotshaw, D. McMorrow, N. Thantu, J. S. Melinger, and R. Kitchenham, "Intermolecular vibrational coherence in molecular liquids," J. Raman Spectrosc. **26**(7), 571–583 (1995).
13. F.-X. d'Abzac, M. Kervella, L. Hespel, and T. Dartigalongue, "Experimental and numerical analysis of ballistic and scattered light using femtosecond optical Kerr gating: a way for the characterization of strongly scattering media," Opt. Express **20**(9), 9604–9615 (2012).
14. P. Yang, L. Liu, and L. Xu, "Dynamic evolution of light-induced orientation of dye-doped liquid crystals in liquid phase studied by time-resolved optically heterodyned optical Kerr effect technique," J. Chem. Phys. **128**(8), 084710 (2008).
15. M. Samoc, J. Swiatkiewicz, and P. N. Prasad, "Dynamics of third-order nonlinearity of canthaxanthin carotenoid by the optically heterodyned phase-tuned femtosecond optical Kerr gate," J. Chem. Phys. **98**(4), 2524–2533 (1993).
16. L. Lin, W. Qian, C. F. Wang, Y. H. Zou, Q. Wang, and H. Y. Chen, "Investigation of third-order nonlinearity of polybenzonitriles by heterodyned femtosecond optical Kerr gate," J. Nonlinear Opt. Phys. Mater. **8**(03), 419–429 (1999).

#225728 - $15.00 USD Received 27 Oct 2014; revised 24 Dec 2014; accepted 8 Jan 2015; published 23 Jan 2015

17. D. McMorrow, W. T. Lotshaw, and G. A. Kenney-Wallace, "Femtosecond optical Kerr studies on the origin of the nonlinear responses in simple liquids," IEEE J. Quantum Electron. **24**(2), 443–454 (1988).
18. P. Zhan, J. Si, W. Tan, X. Liu, B. Wu, S. Xu, F. Chen, and X. Hou, "The influences of turbid media properties on object visibility in optical Kerr gated imaging," Laser Phys. **24**(1), 015401 (2014).
19. C. Calba, L. Méès, C. Rozé, and T. Girasole, "Ultrashort pulse propagation through a strongly scattering medium: simulation and experiments," J. Opt. Soc. Am. A **25**(7), 1541–1550 (2008).

1. Introduction

Ballistic imaging is an optical shadowgraphy technique that is used for improving the visualization of objects hidden in or behind highly turbid media. When an imaging beam transits highly turbid media, most of the beam's photons undergo multiple scattering interactions. These scattered photons follow a considerably more complex pathway in turbid media and seriously degrade the quality of an image in the form of imaging noise. Image-bearing photons consist of ballistic photons and a few slightly scattered snake photons, which go straight though the turbid media and take a shorter pathway than the scattered photons. This phenomenon underlies ballistic imaging, and in particular, the time-gated ballistic imaging technique using an ultrafast optical Kerr gate (OKG) serves as a critical tool to observe objects in highly turbid media [1–4]. In the last few years, this technique has been employed for investigating the dynamics of spray breakup and vaporization in the near field of the liquid-fueled combustion of a high-speed rocket spray [5–7].

In the OKG imaging system, the finite size of the gating beam actually acts as a transient virtual aperture in the Kerr medium for the imaging pulse. To improve the image contrast and signal-to-noise ratio of hidden objects in high turbid media, most OKG imaging systems use the "Kerr-Fourier" imaging configuration to eliminate the scattering photons because the scattering photons belong to the high-spatial-frequency components in the imaging system [4,8,9]. Unfortunately, some high-spatial-frequency components of the detected object were also filtered due to the transient virtual aperture, which leads to poor image sharpness and spatial resolution of the imaging system. Usually, the spatial resolution of the OKG imaging system can be improved by increasing size of the pump beam. However, when the laser power is limited, increasing the size of the pump beam will decrease the power density of the gating beam, which will decrease the imaging intensity and signal-to-noise ratio due to lower OKG transmittance. To avoid the loss of spatial-frequency components and improve the spatial resolution, a collinear, two-color OKG arrangement was proposed in the OKG imaging system [10]. Recently, we also proposed a heterodyned optical Kerr gate (HOKG) imaging method, in which, the spatial resolution of the images can be improved by utilizing a local oscillator signal that contains the high-spatial-frequency components of the object [11]. Moreover, the scattering photons could be effectively eliminated in accordance with the different temporal distribution characteristics of ballistic and scattered photons. Upon increasing the heterodyning angle, the local oscillator signal intensity increases and the sharpness of the image improves. However, a larger number of scattered photons are also introduced into the imaging system as background noise. Therefore, understanding the influence of the heterodyning angle on the imaging quality is important for ballistic imaging applications.

In this study, we investigated the optimum heterodyning angle of the HOKG imaging system. The optimum heterodyning angle for different scattering parameters of a given turbid medium was determined. Moreover, we investigated the dependence of the optimum heterodyning angle on the scattering parameters of the turbid media for HOKG imaging. The experimental results showed that the optimum heterodyning angle varied significantly with increasing optical density (OD) and thickness of the turbid medium.

2. Theory and experimental setup

For HOKG imaging, we assume that the probe beam is initially **x**-polarized in the spatial coordinate system. The analyzer is rotated slightly by a small angle θ from the **y** direction to create a local oscillator field $\sin\theta(E_b(t) + E_s(t))$. Here, $E_b(t)$ and $E_s(t)$ denotes the signal field amplitude of the ballistic and scattered photons of the imaging beam, respectively. According

#225728 - $15.00 USD Received 27 Oct 2014; revised 24 Dec 2014; accepted 8 Jan 2015; published 23 Jan 2015

to the temporal distribution characteristics of ballistic and scattered photons [12,13], the original signal intensity for HOKG imaging is given as [14–17]

$$I_{origin} \propto \int_0^T E^2(t)\,dt + \sin\theta \int_0^T \mathrm{Re}\left[E^*(t)\cdot E_b(t) + E(t)\cdot E_b^*(t)\right]dt + \sin^2\theta\left[\int_0^T E_b^2(t)dt + \int_T^\infty E_s^2(t)dt\right]. \quad (1)$$

Here, $E(t)$ denotes the conventional Kerr signal field amplitude, Re represents the real part of Kerr signal field, T corresponds to the duration of flight of the ballistic photons, and θ denotes the heterodyning angle.

In the Eq. (1), the first term represents the conventional OKG signal and the second term represents heterodyned signal. From the perspective of the imaging information of the object, the first term, which is affected by the transient virtual aperture, only contains the low-spatial-frequency components of the object. On the other hand, the ballistic light field $E_b(t)$ in the second term contains almost all the spatial frequency components of the object. Moreover, the second term is proportional to the product of the ballistic light field $E_b(t)$ and the conventional Kerr signal field $E(t)$. Therefore, HOKG imaging can compensate for the high-spatial-frequency loss that occurs in conventional Kerr imaging. The third term represents the background noise signal ($I_{background} = \sin^2\theta\left[\int_0^T E_b^2(t)dt + \int_T^\infty E_s^2(t)dt\right]$), which can be measured by blocking the gating beam and subtracted. The eventually obtained signal intensity can be rewritten as $I_{signal} \propto \int_0^T E^2(t)\,dt + \sin\theta\int_0^T \mathrm{Re}\left[E^*(t)\cdot E_b(t) + E(t)\cdot E_b^*(t)\right]dt$. We note that the heterodyned signal intensity increases with increase in the heterodyning angle θ. Since the heterodyned signal contains the high-spatial-frequency components of the object, we can expect the image sharpness to improve with increase in the heterodyning angle θ.

In our experiment, we used a Ti: sapphire laser system emitting 50-fs laser pulses centered at 800 nm at a repetition rate of 1 kHz. The output of the laser beam was split into two beams with central wavelengths of about 780 nm and 800 nm. After its transmission through a variable optical delay line, the 780-nm beam was focused onto an optical Kerr medium as the gating beam by a lens. A half-wave plate was introduced in the path of the gating beam to set the angle of the polarization between the pump and the probe beams to $\pi/4$ for maximum gating efficiency.

The 800-nm beam was transmitted through a turbid medium as the imaging beam, which was modulated by a resolution test pattern (United States Air Force contrast target) positioned before the turbid medium. Subsequently, the imaging beam was collected and transmitted through the HOKG setup that consisted of a pair of polarizers and a Kerr material between them. A 1-mm-thick tellurite glass was used as the Kerr medium and positioned at the back focal plane of a collecting lens. By adjusting the optical delay line, the HOKG was opened, and the imaging beam was captured by a CCD camera. The diameter of the gating beam in the Kerr medium was measured to be about 600 μm (intensity decay of $1/e^2$) using a knife-edge method. The full width at half-maximum (FWHM) of the time-resolved optical Kerr signal was measured about 170 fs. In the experiment, the turbid medium samples comprised monodisperse suspensions of 15.0-μm polymethylmethacrylate (PMMA) microspheres, which were contained in a 1-cm-path-length sample cell. The OD of the turbid medium was measured to be about 9.0.

#225728 - $15.00 USD Received 27 Oct 2014; revised 24 Dec 2014; accepted 8 Jan 2015; published 23 Jan 2015

3. Experimental results and discussion

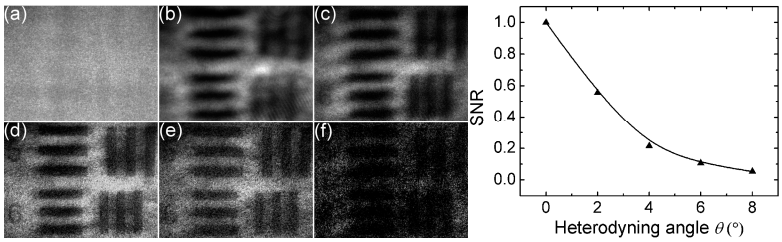

Fig. 1. Comparison of the images of the object under different conditions: (a) direct imaging without the OKG, (b) conventional OKG imaging, (c)–(f) HOKG imaging with different heterodyning angles: (c) 2°, (d) 4°, (e) 6°, and (f) 8°. The dependence of the SNR on the heterodyning angle is shown on the right of Fig. 1.

Figure 1 shows the typical images for the resolution test pattern hidden behind the turbid medium under different conditions. As regards direct imaging, the image of the object was seriously degraded by scattered photons, as shown in Fig. 1(a). As shown in Fig. 1(b), when the heterodyning angle was set to be 0°, namely, as per the conventional OKG imaging arrangement, the boundaries of the shadowed and unshadowed regions were blurred. As mentioned above, this blurring is attributed to the transient virtual aperture induced by the gating beam in the Kerr material, which filters certain high-spatial-frequency components of the object. Because of the compensation of the high-spatial-frequency components of the object provided by the HOKG imaging system, the boundaries of the images can be more clearly identified in Figs. 1(c)-1(f).

Moreover, the image sharpness improved when the heterodyning angle was increased from 2° to 4°, as can be observed from Figs. 1(c) and 1(d). However, the image quality degraded gradually as the heterodyning angle was further increased from 4° to 8°, as can be observed in Figs. 1(d)-1(f). This degradation can be explained as follows: From Eq. (1), we note that the heterodyned signal intensity, which contains the high-spatial-frequency components of the object, increases with increase in the heterodyning angle. However, the background noise signal also increases with increase in the heterodyning angle, corresponding to the third term of the Eq. (1). The signal-to-noise ratio (SNR) for HOKG imaging, which is defined as $I_{signal}/I_{background}$, consequently decreases with increase in the heterodyning angle. When the heterodyning angle was increased to 8°, the SNR measured for our HOKG imaging system nearly reduced to zero, as shown on the right of Fig. 1. Hence, an optimum heterodyning angle should be chosen to ensure sufficient heterodyned signal intensity and to avoid extreme background noise.

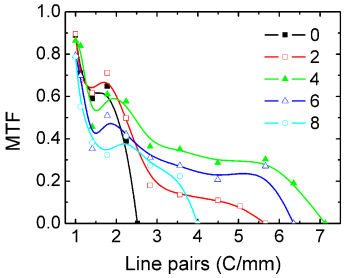

Fig. 2. MTFs of the system measured at different heterodyning angles for HOKG imaging.

Since the performance of the imaging system can be quantitatively evaluated by the modulation transfer function (MTF), we further measured the MTFs for conventional OKG imaging and HOKG imaging at heterodyning angles of 2°, 4°, 6°, and 8°, which results are shown in Fig. 2. For comparison, the MTF for conventional OKG imaging (i.e., the heterodyning angle of 0°) is also shown in Fig. 2. From Fig. 2, we note that the spatial

#225728 - $15.00 USD Received 27 Oct 2014; revised 24 Dec 2014; accepted 8 Jan 2015; published 23 Jan 2015

resolution of the HOKG imaging system increased from 2.2 line pairs per millimeter (lp/mm) to 6.4 lp/mm when the heterodyning angle increased from 0° to 4°. This is because the compensation of the high-spatial-frequency components provided by HOKG imaging of the object increased with increase in the heterodyning angle. However, when the heterodyning angle was further increased from 4° to 8°, the spatial resolution of the HOKG imaging system decreased from 6.4 lp/mm to 3.6 lp/mm due to decrease in the SNR of the imaging system. As a result, the HOKG imaging system's spatial resolution was the highest when the heterodyning angle was set to be 4°. This spatial resolution was 6.4 lp/mm, corresponding to a resolved object size of 78.8 μm. When compared with the HOKG imaging system, the spatial resolution of the conventional OKG imaging system was 2.2 lp/mm, which corresponds to a resolved object size of approximately 222.7 μm. The experimental results indicate that there is an optimum heterodyning angle with which the HOKG imaging system exhibits the highest spatial resolution.

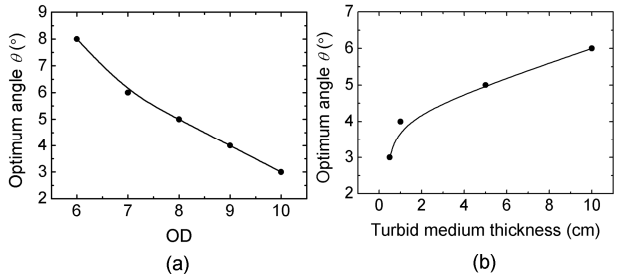

Fig. 3. Optimum heterodyning angle versus the scattering parameters of the turbid medium for HOKG imaging: (a) OD and (b) thickness of the turbid medium.

Previous studies have reported that with regard to light transmitted though turbid media, the proportion of the ballistic photons to scattered photons can be influenced by the scattering parameters [18,19], which can affect the performance of the HOKG imaging system. Thus, we further investigated the dependence of the optimum heterodyning angle on the scattering parameters of the turbid medium for HOKG imaging. Figure 3(a) shows the plot of the optimum heterodyning angle as a function of the OD of the turbid medium for HOKG imaging. The OD of the turbid medium was varied by adjusting the concentrations of the PMMA microsphere suspensions, and the OD value were measured using the collimated transmittance approach with a detection acceptance angle of 0.16°. As shown in Fig. 3(a), the optimum heterodyning angle decreased from 8° to 3° when the OD increased from 6.0 to 10.0. With increase in OD, the background noise signal increased (as can be inferred from Eq. (1)), and as a result, the SNR for HOKG imaging decreased. In general, to obtain a high SNR for dense turbid media, the optimum heterodyning angle of the HOKG imaging system should be decreased. Furthermore, we measured the spatial resolutions of HOKG imaging at the optimum heterodyning angle for different ODs of 6.0, 7.0, 8.0, 9.0, and 10.0, which was about 12.7 lp/mm, 11.3 lp/mm, 10.1 lp/mm, 6.4 lp/mm, and 3.6 lp/mm, respectively. And the corresponding spatial resolution of conventional OKG imaging was about 2.5 lp/mm, 2.2 lp/mm, 2.5 lp/mm, 2.2 lp/mm, and 2.2 lp/mm, respectively. The optimum heterodyning angle decreased with increase in the OD of the turbid medium. Correspondingly, the compensation of the high-spatial-frequency components of the object also decreased, and as a result, the spatial resolution of the HOKG imaging system also decreased with increasing OD. Even so, the spatial resolutions obtained with HOKG imaging were still higher than those with conventional OKG imaging. For example, the spatial resolution of the HOKG imaging system decreased to about 3.6 lp/mm for an OD of 10.0, and the spatial resolution of the conventional OKG imaging system was about 2.2 lp/mm for the same OD.

Figure 3(b) shows the plot of the optimum heterodyning angle as a function of the thickness of the turbid medium for HOKG imaging. The OD of the turbid medium was set to be 8.5 and the thickness of the turbid medium was varied from 0.5 cm to 10 cm in this experiment. From Fig. 3(b), we note that the optimum heterodyning angle increased from 3°

#225728 - $15.00 USD Received 27 Oct 2014; revised 24 Dec 2014; accepted 8 Jan 2015; published 23 Jan 2015

to 6° when the thickness of the turbid medium increased from 0.5 cm to 10 cm. Furthermore, we also measured the spatial resolutions of HOKG imaging at the optimum heterodyning angle for different thickness of 0.5 cm, 1 cm, 5 cm and 10 cm, which was about 3.2 lp/mm, 9.0 lp/mm, 10.1 lp/mm, and 11.3 lp/mm, respectively. And the corresponding spatial resolution of conventional OKG imaging was about 2.2 lp/mm, 2.5 lp/mm, 2.2 lp/mm, and 2.5 lp/mm, respectively. This is because the number of forward-scattered photons traveling through a thicker turbid medium is less than that through a thinner turbid medium at the same OD [18]. These forward-scattered photons are collected as background noise for HOKG imaging. In our study, when the thickness of the turbid medium increased, the background noise signal decreased and the SNR increased. Consequently, the optimum heterodyning angle of the HOKG imaging system for thicker turbid medium is expected to increase. Further, the compensation of the high-spatial-frequency components of the object increased correspondingly. Therefore, the spatial resolution of the HOKG imaging system increased with increasing thickness of the turbid medium, which was higher than that obtained with the conventional OKG imaging system for each case.

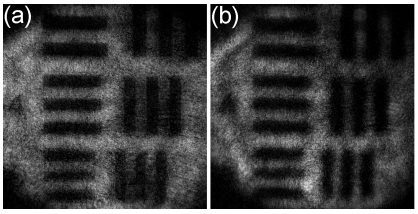

Fig. 4. Comparison of the images using HOKG imaging of different Kerr media: (a) tellurite glass and (b) CS_2.

In addition, we also compared the images using HOKG imaging of the tellurite glass with that of CS_2, and the results are shown in Fig. 4. The turbid medium sample was contained in a 1-cm-path-length sample cell. The OD of the turbid medium was measured to be about 8.5. Both of the optimum heterodyning angles were about 4°. From Fig. 4, we can see that the sharpness of the image for the tellurite glass is higher than that for the CS_2. And the spatial resolution using HOKG imaging of the tellurite glass and CS_2 was about 10.1 lp/mm and 3.2 lp/mm, respectively. This is because when the CS_2 was used as the Kerr medium, some forward-scattered photons cannot be effectively eliminated due to its longer gating time, which weakened the compensation of high-spatial-frequency components of the object.

4. Conclusions

In conclusion, we investigated the influence of the heterodyning angle on HOKG ballistic imaging. Our theoretical analyzing and experiments indicated that an optimum heterodyning angle should be chosen to obtain the best performance of the imaging system. Meanwhile, the scattering parameters of the turbid media also affect the selection of the optimum heterodyning angle. With increase in the OD, the optimum heterodyning angle needs to be significantly decreased in order to avoid increase in the background noise. In addition, when the thickness of the turbid medium increased for a fixed OD, the optimum heterodyning angle increased due to the decreased background noise signal. This research will be useful for ballistic imaging applications.

Acknowledgments

This work was supported by collaborative innovation center of Suzhou nano science and technology. The authors gratefully acknowledge the financial support for this work provided by the National Natural Science Foundation of China under the Grant Nos. 61427816, 61235003, 61308036 and 61205129, and the Natural Science Basic Research Plan in Shaanxi Province of China (Program No. 2014JQ8363).

#225728 - $15.00 USD Received 27 Oct 2014; revised 24 Dec 2014; accepted 8 Jan 2015; published 23 Jan 2015